JPET Fast Forward. Published on March 30, 2021 as DOI: 10.1124/jpet.121.000531
This article has not been copyedited and formatted. The final version may differ from this version.

Brain Concentrations of Methylone and its Metabolites After Systemic Methylone Administration: Relationship to Pharmacodynamic Effects

Nicole Centazzo[1], Michael R. Chojnacki[2], Joshua S. Elmore[2], Raider Rodriguez[1], Teeshavi Acosta[1], Masaki Suzuki[3], Kenner C. Rice[3], Michael H. Baumann[2, *], Marta Concheiro[1, *]

[1]*Department of Sciences, John Jay College of Criminal Justice, City University of New York, New York, NY, USA*

[2]*Designer Drug Research Unit, Intramural Research Program (IRP), National Institute on Drug Abuse (NIDA), National Institutes of Health (NIH), Baltimore, MD, USA*

[3]*Drug Design and Synthesis Section, IRP, NIDA, NIH, Rockville, MD, USA*

** Corresponding authors*

JPET Fast Forward. Published on March 30, 2021 as DOI: 10.1124/jpet.121.000531
This article has not been copyedited and formatted. The final version may differ from this version.

Running Title: Methylone Brain Concentrations and Pharmacodynamic Effects

Corresponding and co-corresponding authors' contact information:
Michael H. Baumann, Ph.D.
Chief, Designer Drug Research Unit (DDRU)
IRP, NIDA, NIH, DHHS
333 Cassell Drive, Suite 4400
Baltimore, MD 21224
Phone: 443-740-2660
Email: mbaumann@mail.nih.gov

Marta Concheiro, Ph.D.
Assistant Professor in Toxicology
Department of Sciences
John Jay College of Criminal Justice
City University of New York
524 West 59th Street – Rm 5.66.02
New York, NY 10019
Phone: 212-237-8492
Email: mconcheiro-guisan@jjay.cuny.edu

Number of text pages: 18
Number of tables: 3 (+ 4 supplemental tables)
Number of figures: 11
Number of references: 32
Number of words in the Abstract: 247
Number of words in the Introduction: 699
Number of words in the Discussion: 1492

JPET Fast Forward. Published on March 30, 2021 as DOI: 10.1124/jpet.121.000531
This article has not been copyedited and formatted. The final version may differ from this version.

List of nonstandard abbreviations:

5-HIAA: 5-hydroxyindoleacetic acid
DEA: US Drug Enforcement Administration
DOPAC: 3,4-dihydroxyphenylacetic acid
EDTA: ethylenediaminetetraacetic acid
HHMC: 3,4-dihydroxy-*N*-methylcathinone
HMMC: 4-hydroxy-3-methoxy-*N*-methylcathinone
HPLC-ECD: high-performance liquid chromatography with electrochemical detection
HVA: homovanillic acid
IRP: Intramural Research Program
LC-MS: liquid chromatography–mass spectrometry
LC-MSMS: liquid chromatography-tandem mass spectrometry
LOQ: limits of quantification
MDMA: 3,4-methylenedioxy-*N*-methylamphetamine
MDC: 3,4-methylenedioxycathinone
MDMC: methylone
MDPV: 3,4-methylenedioxypyrovalerone
MRM: multiple reaction monitoring
NPS: new psychoactive substances
SMBS: sodium metabisulfite

JPET Fast Forward. Published on March 30, 2021 as DOI: 10.1124/jpet.121.000531
This article has not been copyedited and formatted. The final version may differ from this version.

Abstract

3,4-Methylenedioxy-*N*-methylcathinone (methylone) is a new psychoactive substance with stimulant properties and potential for abuse. Despite its popularity, limited studies have examined relationships between brain concentrations of methylone, its metabolites, and pharmacodynamic effects. The goal of the present study was two-fold: 1) to determine pharmacokinetics of methylone and its major metabolites, 4-hydroxy-3-methoxy-*N*-methylcathinone (HMMC), 3,4-dihydroxy-*N*-methylcathinone (HHMC), and 3,4-methylenedioxycathinone (MDC) in rat brain and plasma; 2) to relate brain pharmacokinetic parameters to pharmacodynamic effects including locomotor behavior and post-mortem neurochemistry. Male Sprague-Dawley rats received s.c. methylone (6, 12, or 24 mg/kg) or saline vehicle (n=16/dose), and subgroups were decapitated after 40 or 120 min. Plasma and prefrontal cortex were analyzed for concentrations of methylone and its metabolites by liquid chromatography-tandem mass spectrometry. Frontal cortex and dorsal striatum were analyzed for dopamine, 5-HT, and their metabolites by high-performance liquid chromatography-electrochemical detection. Brain and plasma concentrations of methylone and its metabolites rose with increasing methylone dose, but brain methylone and MDC concentrations were greater than dose-proportional. Brain-to-plasma ratios for methylone and MDC were $\geq$3 (range 3-12), whereas those for HHMC and HMMC were $\leq$0.2 (range 0.01-0.2). Locomotor activity score was positively correlated with brain methylone and MDC, whereas cortical 5-HT was negatively correlated with these analytes at 120 min. Our findings show that brain concentrations of methylone and MDC display non-linear accumulation. Behavioral and neurochemical effects of systemically administered methylone are related to brain concentrations of methylone and MDC, but not its hydroxylated metabolites, which do not effectively penetrate into the brain.

JPET Fast Forward. Published on March 30, 2021 as DOI: 10.1124/jpet.121.000531
This article has not been copyedited and formatted. The final version may differ from this version.

Significance Statement

Behavioral and neurochemical effects of methylone are related to brain concentrations of methylone and its metabolite MDC, but not its hydroxylated metabolites, HMMC and HHMC, which do not effectively penetrate into the brain. Methylone and MDC display non-linear accumulation in the brain, which could cause untoward effects on 5-HT neurons in vulnerable brain regions, including the frontal cortex.

JPET Fast Forward. Published on March 30, 2021 as DOI: 10.1124/jpet.121.000531
This article has not been copyedited and formatted. The final version may differ from this version.

Introduction

In the past decade, non-medical (i.e., recreational) drug markets worldwide have seen an increase in the availability of stimulant-like new psychoactive substances (NPS), including synthetic cathinones. These substances are chemically similar to amphetamines, and they have been sold as "bath salts" or "research chemicals" to evade drug control legislation in the United States (US) and elsewhere (Baumann *et al.*, 2013; Madras, 2016). In 2011, the most prevalent synthetic cathinones - methylone, mephedrone, and 3,4-methylenedioxypyrovalerone (MDPV) - were placed into emergency Schedule I control by the US Drug Enforcement Administration (DEA), and the substances were permanently scheduled in 2013 (Drug Enforcement Administration (DEA), 2013). The first forensic identifications of methylone occurred in 2009 with 4 case reports, but serious drug exposures increased markedly in the following years, reaching a peak of 3,976 case reports in 2013 (Drug Enforcement Administration (DEA), 2019). In more recent times, methylone and its analogs (e.g., pentylone) are found as adulterants in counterfeit *Ecstasy* pills sold as the club drug 3,4-methylenedioxy-*N*-methylamphetamine (MDMA), and therefore, many drug users consume these compounds unknowingly (Oliver *et al.*, 2019).

Methylone is the β-keto analog of MDMA, and not surprisingly, it produces similar pharmacological effects to MDMA (De Felice *et al.*, 2014; Baumann *et al.*, 2018). More specifically, methylone acts as a substrate-type releasing agent at high-affinity transporters for dopamine, norepinephrine, and 5-HT in rat brain tissue and in cells transfected with human transporters (Baumann *et al.*, 2012; Eshleman *et al.*, 2013; Simmler *et al.*, 2013). The monoamine-releasing effects of methylone produce elevations in extracellular dopamine and 5-HT in brain reward pathways, as measured by *in vivo* microdialysis (Schindler *et al.*, 2016;

JPET Fast Forward. Published on March 30, 2021 as DOI: 10.1124/jpet.121.000531
This article has not been copyedited and formatted. The final version may differ from this version.

Elmore *et al.*, 2017). Drug self-administration studies in rats demonstrate that methylone exhibits reinforcing properties, which suggests the drug has abuse potential (Watterson *et al.*, 2012; Vanderwater *et al.*, 2015).

In humans, methylone is metabolized by cytochrome P450 2D6 (CYP2D6), with minor contributions from CYP1A2, CYP2B6, and CYP2C19 (Pedersen *et al.*, 2013), whereas in rats, the precise cytochrome(s) responsible are not well established but might involve CYP2D1, the rat isoform of CYP2D6 (Malpass *et al.*, 1999). Similar to MDMA, methylone is metabolized via two distinct pathways in the liver (see Figure 1): 1) *O*-demethylenation to form 3,4-dihydroxy-*N*-methylcathinone (HHMC), which is rapidly converted to 4-hydroxy-3-methoxy-*N*-methylcathinone (HMMC), and 2) *N*-demethylation to form 3,4-methylenedioxycathinone (MDC) or normethylone. It is noteworthy that HMMC is the predominant metabolite of methylone in blood and plasma from both rats and humans. Phase II metabolism includes the formation of glucuronide and sulfate conjugates of the hydroxylated metabolites HHMC and HMMC (Kamata *et al.*, 2006; Meyer *et al.*, 2010). Our previous studies show that certain phase I methylone metabolites are bioactive (Elmore *et al.*, 2017; Luethi *et al.*, 2019). MDC and HHMC are substrate-type releasers at monoamine transporters *in vitro*, but only MDC produces significant elevations in brain extracellular dopamine and 5-HT *in vivo*. The reason why HHMC lacks bioactivity *in vivo* is not known but could be related to poor penetration across the blood-brain barrier, due to its rapid conjugation in the bloodstream or higher polarity when compared to methylone.

- *Insert Figure 1 here* -

JPET Fast Forward. Published on March 30, 2021 as DOI: 10.1124/jpet.121.000531
This article has not been copyedited and formatted. The final version may differ from this version.

Severe clinical side effects have been reported from the misuse of methylone, such as aggressive behavior, psychosis, hyperthermia, seizures, and even death (Cawrse *et al.*, 2012; Ellefsen *et al.*, 2015), but limited studies have examined relationships between methylone pharmacokinetics, metabolism, and its pharmacodynamic effects. Controlled administration studies with methylone and other NPS in humans are limited due to ethical constraints, so pharmacokinetic studies in animal models fill a critical void. Several research groups have investigated the pharmacokinetics and pharmacodynamics of methylone in rodent models (López-Arnau *et al.*, 2013; Elmore *et al.*, 2017; Grecco *et al.*, 2017; Štefková *et al.*, 2017). In particular, Lopez-Arnau and colleagues (López-Arnau *et al.*, 2013) examined pharmacokinetics of methylone in rats, and their findings suggest that metabolites may contribute to pharmacodynamic effects of the drug *in vivo*. Given the aforementioned information, the goal of the present study was two-fold: 1) to determine the pharmacokinetics of methylone and its three major metabolites - HMMC, HHMC, MDC - in rat brain and plasma; 2) to relate brain pharmacokinetic parameters to acute pharmacodynamic effects including locomotor behavior and post-mortem neurochemistry.

Materials and Methods

Drugs, Chemicals, and Reagents

(±)-3,4-Methylenedioxy-*N*-methylcathinone (methylone) for animal studies was acquired from the National Institute on Drug Abuse (NIDA), Drug Supply Program (Rockville, MD, USA). For analytical procedures, methylone (1 mg/mL in methanol) and its deuterated standard methylone-d_3 (100 μg/mL in methanol) were obtained from Cerilliant (Round Rock, TX, USA).

JPET Fast Forward. Published on March 30, 2021 as DOI: 10.1124/jpet.121.000531
This article has not been copyedited and formatted. The final version may differ from this version.

As reported by Ellefsen et al. (Ellefsen *et al.*, 2015), the methylone metabolites, MDC, HHMC, and HMMC were synthesized and purified by the Drug Design and Synthesis Section of the NIDA Intramural Research Program (IRP) (Baltimore, MD, USA). The monoamine standards for dopamine, 3,4-dihydroxyphenylacetic acid (DOPAC), homovanillic acid (HVA), 5-HT, and 5-hydroxyindoleacetic acid (5-HIAA) were obtained from Sigma-Aldrich (St. Louis, MO, USA).

Liquid chromatography–mass spectrometry (LC-MS) grade acetonitrile, ethylenediaminetetraacetic acid (EDTA), formic acid, isopropanol, methanol, and sodium metabisulfite (SMBS) were obtained from Thermo Fisher Scientific (Fair Lawn, NJ, USA). BG100® liquid β-glucuronidase from Red Abalone *Haliotis rufescens* (>100 KU/mL) was purchased from Kura Biotec (Inglewood, CA, USA) and 4-methylcatechol from Sigma-Aldrich (Milwaukee, WI, USA). Hydrochloric acid (HCl) 36.5-38% was obtained from J.T. Baker Chemical Company (Phillipsburg, NJ, USA). Brains from drug-naïve male Sprague Dawley rats were acquired from BioIVT (Hicksville, NY, USA) and used for development of the method to quantify methylone in brain tissue. Two-mL 1.4 mm ceramic beads were obtained from Thermo Fisher Scientific (Fair Lawn, NJ, USA) and 10-mL 100 x 16 mm polypropylene tubes were purchased from Sarstedt Inc. (Newton, NC, USA).

Animals, Dosing Regimen, and Tissue Collection

Male Sprague-Dawley rats (300-400 g), purchased from Envigo (Frederick, MD, USA), were double-housed under conditions of controlled temperature (22 ± 2ºC) and humidity (45 ± 5%), with *ad libitum* access to food and water. Lights were on between 7:00 AM and 7:00 PM. The Institutional Animal Care and Use Committee of the NIDA IRP approved the animal experiments, and all procedures were carried out in accordance with the National Institutes of

Health Guide for the Care and Use of Laboratory Animals. Vivarium facilities were fully accredited by the Association for Assessment and Accreditation of Laboratory Animal Care. Experiments were designed to minimize the number of animals included in the study.

One week prior to drug treatments, rats were single-housed. On the day of the experiment, groups of rats received s.c. methylone (6, 12, or 24 mg/kg) or its saline vehicle (n=16/dose) and were returned to their home cages; subgroups were subsequently killed by decapitation at 40 min or 120 min post-injection. These particular time points were chosen for tissue collection based on our previous study which showed plasma MDC concentrations peak at 30-40 min post-injection, while plasma HMMC concentrations peak much later at 90-120 min (Elmore *et al.*, 2017). Injections were carried out in the vivarium, whereas decapitation was carried out in a separate necropsy room. Trunk blood was collected, brains were rapidly removed from the skull, and tissue from prefrontal cortex, frontal cortex, and dorsal striatum was dissected on ice. Plasma and brain tissue were stored frozen at -80°C until the time of analysis.

Assessment of Locomotor Behavior and Body Temperature

Just prior to decapitation, each rat was observed for 1 min in its home cage to discern locomotor behavior, and core body temperature was measured. Behavior was scored using a numerical scale: 1 = asleep or still; 2 = in-place activities; 3 = locomotion, rearing, or sniffing; 4 = any two (locomotion, rearing, or sniffing); 5 = 10 s of continuous sniffing without locomotion or rearing; 6 = 10 s of continuous sniffing with locomotion or rearing; 7 = 5 s of patterned sniffing; 8 = 10 s of patterned sniffing. Patterned sniffing was defined as any repeated head motion (e.g., up and down 'head bobbing') that occurred simultaneously with sniffing behavior. This behavioral scale is sensitive to dose-related changes in motor activation caused by

JPET Fast Forward. Published on March 30, 2021 as DOI: 10.1124/jpet.121.000531
This article has not been copyedited and formatted. The final version may differ from this version.

psychomotor stimulants (Baumann *et al.*, 1993; Elmore *et al.*, 2017). The behavioral observer was blinded to the experimental condition. After the observation period, rats were removed from their cages and core body temperature was measured via insertion of a RET-2 probe (Physitemp Instruments, Clifton, NJ, USA) into the colon. Rats were then transported in their home cages to the necropsy room where they were decapitated.

Monoamine and Metabolite Analysis in Rat Brain

Brain tissue from the frontal cortex and dorsal striatum was analyzed for dopamine, DOPAC, HVA, 5-HT, and 5-HIAA via high-performance liquid chromatography with electrochemical detection (HPLC-ECD). Tissue samples were weighed, homogenized by ultra-sonication in 0.1 N perchloric acid, and centrifuged at 16,600 x g for 18 min at 4ºC in an Eppendorf 5415R refrigerated centrifuge by Marshall Scientific (Hampton, NH, USA). Aliquots of the supernatant were injected onto a Sunfire C18 HPLC column (150 x 4.6 mm, 3.5 µm particles, 100 Å pore size) (Waters Millipore, Milford, MA, USA) linked to a coulometric detector (ESA Model Coulochem III, Dionex, Chelmsford, MA, USA). Mobile phase consisting of 50 mM sodium phosphate monobasic, 250 µM Na_2EDTA, 0.03% sodium octane sulfonic acid, and 25% methanol (pH = 2.75) was recirculated at 0.9 mL/min. Known monoamine standards, ranging in concentration from 10 to 1,000 pg/µL, were assayed along with each set of samples. Data were acquired by a Waters Empower software system (Waters Millipore), where peak heights of unknowns were compared with those of standards. The lower limit of assay sensitivity (3× baseline noise) was 30 pg/20 µL sample.

Methylone and Metabolites Analysis in Rat Plasma

JPET Fast Forward. Published on March 30, 2021 as DOI: 10.1124/jpet.121.000531
This article has not been copyedited and formatted. The final version may differ from this version.

Plasma samples were analyzed by liquid chromatography-tandem mass spectrometry (LC-MSMS) as previously described by Ellefsen et al. (Ellefsen *et al.*, 2015). Specifically, 20 µL of 250 mM SMBS, 10 µL of 250 mM EDTA, 50 µL of internal standard (methylone-d_3) at 100 ng/mL, and 100 µL rat plasma were mixed in 1.5-mL microcentrifuge tubes and gently vortexed. After enzymatic hydrolysis (10 µL of β-glucuronidase, incubation at 50°C, one hour), 20 µL of 4-methylcathechol and 10 µL of perchloric acid were mixed with each sample. The samples were extracted using mixed-mode cation exchange solid phase extraction. The eluent was acidified with 100 µL of 1% HCl in methanol and evaporated to dryness in a Turbovap® (Biotage, Charlotte, NC, USA). Two hundred µL of 0.1% formic acid in water was utilized for reconstitution, and the solution was transferred to injection vials. A LC-MSMS system, with a Nexera UHPLC system coupled to a triple quadrupole LCMS-8050 from Shimadzu (Columbia, MD, USA), was employed for the instrumental analysis. The chromatographic separation was performed using a Synergi Polar-RP LC column (100 x 2 mm, 2.5µm particles, 100Å pore size) (Phenomenex, Torrance, CA, USA), and the mobile phase in gradient mode was a combination of 0.1% formic acid in water (mobile phase A) and 0.1% formic acid in acetonitrile (mobile phase B). Mass spectrometer data were collected in positive electrospray ionization mode with two multiple reaction monitoring (MRM) transitions per analyte (Supplemental Table S1). The method was linear from 0.5 (methylone, HMMC and MDC) or 10 (HHMC) to 1,000 ng/mL. Validation details are described in Ellefsen et al. (Ellefsen *et al.*, 2015). If a plasma sample was quantified above the upper limit of quantification (1,000 ng/mL), the sample was diluted 1:10 with blank rat plasma, and reanalyzed. Once the diluted sample was quantified within the calibration range, the final concentration was obtained by multiplying the measured concentration of the diluted sample by the dilution factor.

JPET Fast Forward. Published on March 30, 2021 as DOI: 10.1124/jpet.121.000531
This article has not been copyedited and formatted. The final version may differ from this version.

Methylone and Metabolites Analysis in Rat Brain

Prefrontal cortical tissue from each rat was weighed and transferred into a bead mill tube containing ceramic beads and 500 µL of 7.5 mM SMBS, 7.5 mM EDTA in 10 mM formic acid (SMBS-EDTA-FA mixture). The samples were homogenized on a Bead Ruptor Elite bead mill homogenizer by OMNI International (Kennesaw, GA, USA). The homogenization program consisted of one cycle lasting 20 s at a speed of 4.85 m/s. After centrifugation (6,200 x g, 5 min), 25 µL internal standard (methylone-d_3) at 100 ng/mL was added and the enzymatic hydrolysis was performed (10 µL of β-glucuronidase, incubation at 50℃, one hour). After adding 20 µL of 4-methylcatechol to each sample, 800 µL of cold acetonitrile was used for protein precipitation. One hundred µL of 1% HCl in methanol was added to the supernatant and samples were evaporated to dryness. Reconstitution was performed by adding 200 µL of MP-A, and the sample was transferred into a nanoFilter Vial® 0.2 µm PVDF with red screw cap (Thomson Instrument Company, Oceanside, CA, USA), before being analyzed by LC-MSMS as described for the plasma samples (injection volume 20 µL). The method was linear from 5 to 1,000 ng/g for all compounds. Validation parameters are summarized in Supplemental Tables S2-S4. If a brain sample quantified above the upper limit of quantification (1,000 ng/g), the brain homogenate was diluted at 1:10 or 1:100 with the SMBS-EDTA-FA mixture, and reanalyzed. Once the diluted sample quantified within the calibration range, the final concentration was obtained by multiplying the measured concentration of the diluted sample by the dilution factor.

Data Analysis and Statistics

JPET Fast Forward. Published on March 30, 2021 as DOI: 10.1124/jpet.121.000531
This article has not been copyedited and formatted. The final version may differ from this version.

Data collected from the analysis of drug and metabolite concentrations, locomotor activity scores, body temperature, and neurotransmitter levels were tabulated, analyzed and graphed with GraphPad Prism (version 7, GraphPad Software, La Jolla, CA, USA). For the pharmacokinetic findings, two-way ANOVA (dose x matrix) followed by Sidak's multiple comparison test was performed to compare plasma versus brain concentrations of analytes. As a means to assess the potential for non-linear accumulation of analytes, two-way ANOVA (dose x condition) followed by Sidak's test was used to compare predicted versus observed brain concentrations of methylone and MDC at each time point. Predicted brain concentrations at the 12 and 24 mg/kg doses were calculated by multiplying measured analyte concentrations after 6 mg/kg methylone by a factor of 2 and 4, respectively. Pharmacodynamic findings were examined by one-way ANOVA (dose), followed by Bonferroni's post-hoc test. A correlation matrix, which included brain concentrations of methylone and MDC, neurotransmitter levels from the frontal cortex and dorsal striatum, locomotor activity scores, and core temperature, was created and subsequently analyzed by Pearson's tests and linear regression analyses. In all the statistical analyses, $p<0.05$ was considered significant.

Results

Pharmacokinetics of Methylone and its Metabolites

A total of 48 brain and plasma samples from rats receiving s.c. methylone (3 doses), collected at 40 min or 120 min post-injection (2 time points), were analyzed with the described LC-MSMS procedure (n=8 rats/dose at each time point). The limits of quantification (LOQ) in brain and plasma were 5 ng/g and 0.5 ng/mL, with the exception of HHMC in plasma, which displayed an LOQ of 10 ng/mL. The plasma concentrations of analytes are summarized in Table

JPET Fast Forward. Published on March 30, 2021 as DOI: 10.1124/jpet.121.000531
This article has not been copyedited and formatted. The final version may differ from this version.

1, whereas brain concentrations are summarized in Table 2. In general, concentrations of methylone and its metabolites increased in both matrices as the dose administered was increased.

- *Insert Figure 2 here* –

Figure 2 depicts the brain and plasma concentrations of methylone and MDC at the 40-min and 120-min time points. A two-way ANOVA (dose x matrix) comparing brain and plasma concentrations of methylone at 40 min revealed significant main effects of dose ($F_{2,42}$=27.09, p<0.0001) and matrix ($F_{1,42}$=75.19, p<0.0001), with a significant dose x matrix interaction ($F_{2,42}$=17.85, p<0.0001). Similar results were found for methylone measures at 120 min. At all doses and time points, brain concentrations of methylone were far greater than plasma concentrations. A two-way ANOVA comparing brain and plasma concentration of MDC at 40 min revealed significant effects of dose ($F_{2,42}$=21.62, p<0.0001) and matrix ($F_{1,42}$=58.40, p<0.001), with a significant dose x matrix interaction ($F_{2,42}$=9.932, p<0.003). Similar results were found for MDC measures at 120 min. At all doses and time points, brain concentrations of MDC exceeded those measured in plasma. Figure 3 illustrates the brain and plasma concentrations of the hydroxylated metabolites HHMC and HMMC. In contrast to the findings for methylone and MDC, brain concentrations of HHMC and HMMC were extremely low in all tissue samples. A two-way ANOVA comparing the brain and plasma concentration of HHMC at 40 min revealed significant effects of dose ($F_{2,42}$=25.90, p<0.0001) and matrix ($F=_{1,42}$=244.6), with a significant dose x matrix interaction ($F_{2,42}$=21.18, P<0.0001). Similar results were found for HHMC at 120 min. At all doses and time points, plasma concentrations of HHMC were significantly greater than brain concentrations. A two-way ANOVA comparing brain and plasma

JPET Fast Forward. Published on March 30, 2021 as DOI: 10.1124/jpet.121.000531
This article has not been copyedited and formatted. The final version may differ from this version.

concentration of HMMC at 40 min revealed significant effects of dose ($F_{2,41}$=56.73, p<0.0001) and matrix ($F_{1,41}$=694, p<0.0001), with a significant dose x matrix interaction ($F_{2,41}$=26.98, p<0.0001). Similar results were found for HMMC at 120 min. At all doses and time points, plasma concentrations of HMMC far exceeded those measured in brain.

- *Insert Figure 3 here* -

The data in Table 3 summarize brain-to-plasma ratios for all analytes. Methylone and MDC displayed brain-to-plasma ratios $\geq$3 (range 3-14), whereas HHMC and HMMC had ratios $\leq$0.2 (range of 0.01-0.2). These results confirm that methylone and its *N*-demethylated metabolite MDC freely cross the blood-brain-barrier to reach the brain, whereas HHMC and HMMC do not. To investigate the possible reasons underlying the lack of hydroxylated metabolites reaching the brain, we explored the presence of glucuronide or sulfate conjugates in both plasma and brain. Briefly, we compared analyte concentrations in plasma and brain samples which were subjected to 2 separate analytical procedures, one that involved sample hydrolysis to cleave conjugated metabolites and another that did not. In the brain, no phase II metabolites were detected for any of the metabolites. In plasma, HMMC and HHMC were mainly present as conjugates. The percentage of HMMC in conjugated form ranged from 47.6 to 95.7%, median 84.6%, and the percentage of HHMC as conjugated metabolite ranged from 49.2 to 99.8%, median 87.6%. These results show that HHMC and HMMC are predominantly present as conjugates in plasma, and these conjugates do not cross the blood-brain barrier.

Data from our previous study suggested that methylone concentrations in plasma may exhibit non-linear accumulation, where circulating drug concentrations are greater than dose-

JPET Fast Forward. Published on March 30, 2021 as DOI: 10.1124/jpet.121.000531
This article has not been copyedited and formatted. The final version may differ from this version.

proportional (Elmore *et al.*, 2017). Therefore, we compared the predicted concentrations of methylone and MDC in brain tissue to their actual observed concentrations. Data in Figure 4 show the predicted versus observed concentrations for methylone and MDC in brain. A two-way ANOVA (dose x condition) comparing predicted versus observed brain concentrations of methylone at the 40-min time point revealed significant main effects of dose ($F_{2,42}$=32.49, $p<0.0001$) and condition ($F_{1,42}$=6.05, $p<0.01$), where observed methylone concentrations were significantly greater than predicted at the 24 mg/kg methylone dose ($p<0.05$ Sidak's test). Similar results were found for the 120-min time point, where the observed concentration of methylone was significantly greater than the predicted concentration at 24 mg/kg dose. A two-way ANOVA comparing the predicted versus observed brain concentrations of MDC at the 40-min time point revealed significant main effects of dose ($F_{2,42}$=29.45, $p<0.001$) and condition ($F_{1,42}$=5.93, $p<0.01$), but the predicted and observed concentrations did not differ significantly at any dose. A similar analysis of MDC concentrations at 120 min found significant main effects of dose ($F_{2,42}$=64.36, $p<0.0001$) and condition ($F_{1,42}$=38.34, $p<0.0001$), where the observed concentrations were significantly greater than predicted at the 12 and 24 mg/kg doses. The findings with MDC suggest that there is a delayed accumulation of this analyte in the brain.

- Insert Figure 4 here –

- Insert Figure 5 here -

Pharmacodynamic Effects of Methylone

The effects of methylone on core body temperature and locomotor behavioral score are shown in Figure 5. Methylone administration affected temperature in a dose- and time-dependent

JPET Fast Forward. Published on March 30, 2021 as DOI: 10.1124/jpet.121.000531
This article has not been copyedited and formatted. The final version may differ from this version.

manner, with initial hypothermia followed by delayed hyperthermia. A one-way ANOVA (dose) for temperature data demonstrated that methylone significantly affected body temperature at the 40-min time point ($F_{3,28}$=11.90, p<0.0001), with modest hypothermia occurring after the 6 and 12 mg/kg doses. At the 120-min time point, methylone significantly affected temperature ($F_{3,28}$=5.734, p<0.003), with a modest but significant hyperthermia of about 0.5^{o}C above normal, observed at the 12 and 24 mg/kg doses. Methylone administration significantly altered locomotor score at both 40 min ($F_{3,28}$=56.36, p<0.0001) and 120 min ($F_{3,28}$=36.55, p<0.0001). At both time points, Bonferroni's post hoc test revealed significant increases in behavioral score after the 6, 12, and 24 mg/kg doses when compared to saline control. Figure 6 depicts the effects of methylone on post-mortem concentrations of 5-HT and dopamine in the frontal cortex. Methylone did not affect 5-HT at 40 min, but significantly influenced 5-HT at 120 min ($F_{3,28}$=33.88, p<0.0001), with substantial dose-related decreases in 5-HT, which reached 60% reduction at the 24 mg/kg dose. Methylone failed to alter dopamine concentrations in the frontal cortex. Figure 7 shows the effects of methylone on post-mortem tissue 5-HT and dopamine in the dorsal striatum. Methylone had no effect on striatal 5-HT at either time point. By contrast, methylone slightly, albeit significantly, elevated striatal dopamine at both the 40-min ($F_{3,28}$=3.73, p<0.02) and 120-min ($F_{3,28}$=7,29, p<0.001) time points.

- Insert Figure 6 here -

- Insert Figure 7 here -

Correlative Relationships

JPET Fast Forward. Published on March 30, 2021 as DOI: 10.1124/jpet.121.000531
This article has not been copyedited and formatted. The final version may differ from this version.

We obtained pharmacokinetic and pharmacodynamic data from the same experimental subjects, which allowed us to examine potential correlative relationships among various endpoints. We were particularly interested in the relationship between brain analyte concentrations and pharmacodynamic effects. The present pharmacokinetic findings revealed the absence of hydroxylated metabolites in the brain, so all correlation analyses were confined to brain concentrations of methylone and MDC. Figure 8 depicts the correlations between brain concentrations of methylone and body temperature or behavioral score. At the 40-min time point, brain methylone was positively correlated with both temperature (Pearson's $r=0.6751$, $p<0.0005$) and behavioral score ($r=0.6985$, $p<0.0001$). At 120 min, methylone was not correlated with temperature ($r=0.3567$, NS) but did correlate with behavioral score ($r=0.7841$, $p<0.0001$). Figure 9 shows that brain MDC concentrations were positively correlated with body temperature ($r=0.6118$, $p<0.0015$) and behavioral score ($r=0.6688$, $p<0.0004$) at 40 min post-injection, and similar positive correlations were observed at the 120-min time point.

- Insert Figure 8 here -

- Insert Figure 9 here -

Figure 10 illustrates the correlations between brain methylone concentration and cortical 5-HT or dopamine. Brain concentrations of methylone did not correlate with either cortical neurotransmitter at 40 min. However, at the 120 min time point, methylone was negatively correlated with cortical 5-HT ($r=-0.6701$, $p<0.0003$). Figure 11 shows the correlations between MDC concentrations and cortical 5-HT or dopamine. Brain concentrations of MDC did not correlate with either neurotransmitter at the 40 min time point, but at 120 min, there was a

JPET Fast Forward. Published on March 30, 2021 as DOI: 10.1124/jpet.121.000531
This article has not been copyedited and formatted. The final version may differ from this version.

significant negative correlation between MDC and 5-HT ($r=-0.7597$, $p<0.0001$). No correlations were found when examining relationships among methylone, MDC, and striatal neurotransmitters.

- Insert Figure 10 here -

- Insert Figure 11 here -

Discussion

A primary aim of the present study was to quantify brain and plasma concentrations of methylone and its metabolites after systemic methylone administration to male rats. In general, methylone and metabolite concentrations rose in parallel with increasing dose of methylone administered, but brain methylone and MDC concentrations were greater than dose-proportional at the highest dose administered. Methylone and MDC displayed brain-to-plasma ratios ≥ 3 (range 3-12) whereas HHMC and HMMC had brain-to-plasma ratios ≤ 0.2 (range 0.01-0.2). These findings demonstrate that methylone and MDC freely penetrate into the central nervous system, but hydroxylated metabolites do not. A secondary aim of the study was to relate brain analyte concentrations with acute pharmacodynamic effects of methylone. In this regard, locomotor activity score was positively correlated with brain concentrations of methylone and MDC, while post-mortem 5-HT levels in the cortex were negatively correlated with these same analytes. Overall, the findings show that acute pharmacodynamic effects of methylone are likely related to brain concentrations of the parent compound and its *N*-demethylated metabolite.

It is notable that we found evidence for non-linear accumulation of methylone and MDC in the brain. Elmore et al. (Elmore *et al.*, 2017) reported non-linear kinetics for methylone in

plasma, while López-Arnau et al. (López-Arnau *et al.*, 2013) found no evidence for the phenomenon. Here, we report the first dose-effect investigation of methylone and metabolite concentrations in the brain. The doses of methylone we employed were chosen based on our previous study (Elmore *et al.*, 2017), where we observed higher than predicted concentrations of methylone in plasma after s.c. administration of 12 mg/kg. The current findings show that non-linear accumulation of methylone and MDC occurs in the brain at higher drug doses, and this effect is more robust after 120 min compared to 40 min. Our data are consistent with the notion that methylone induces a dose- and time-dependent inhibition of CYP2D1 (the rat isoform of CYP2D6 in humans), the chief enzyme responsible for biotransformation of methylone. Indeed, Pedersen et al. (Pedersen *et al.*, 2013) found that methylone inhibits CYP2D6 with a Ki of 15 µM, which translates to ~3,000 ng/g, a concentration that is achieved in rat brain tissue after the 12 and 24 mg/kg doses of methylone (see Table 2). We hypothesize that methylone is capable of inactivating CYP2D1 in rats, in a manner analogous to the effect of MDMA on CYP2D6 in humans (de la Torre *et al.*, 2004), and subsequent studies should address this hypothesis. From a clinical perspective, the non-linear kinetics of methylone might be a contributing factor to the adverse effects of the drug reported after high-dose exposure in humans (Cawrse *et al.*, 2012; Ellefsen *et al.*, 2015). Similar toxicities have been reported in rats self-administering large doses of methylone (Gannon *et al.*; 2018; Gannon *et al.*; 2019).

The collection of brain tissue and plasma from the same rats made it possible to determine brain-to-plasma ratios for methylone and its metabolites. Our results reveal that methylone and MDC are readily able to cross the blood-brain-barrier (brain-to-plasma ratios from 3-14), while HHMC and HMMC do not (brain-to-plasma ratio from 0.01 to 0.2). In fact, the small amounts of HHMC and HMMC detected in brain were likely related to analyte

JPET Fast Forward. Published on March 30, 2021 as DOI: 10.1124/jpet.121.000531
This article has not been copyedited and formatted. The final version may differ from this version.

concentrations in residual blood found in post-mortem brain tissue samples. Limited information is available about the distribution of methylone and its metabolites in the brain or other organs (Štefková *et al.*, 2017). Lopez-Arnau et al. (López-Arnau *et al.*, 2013) reported a methylone brain-to-plasma ratio of 1.42 after an oral dose of 30 mg/kg methylone. In that study, the oral route of administration might explain lower concentrations of drug reaching the brain, secondary to extensive gut and hepatic metabolism of the parent compound. Stefkova et al. (Štefková *et al.*, 2017) reported that s.c. methylone administration yields a brain-to-serum ratio of 7.97 whereas Grecco et al. (Grecco *et al.*, 2017) found that s.c. methylone yields a brain-to-plasma ratio of 39.5. It is noteworthy that the latter finding was based on area-under-curve estimates rather than single time points. Regardless of the details, all of the available data from rats agree that methylone and MDC freely cross the blood-brain-barrier. In contrast to methylone and MDC, we show that HHMC and HMMC are found at particularly low concentrations in the brain. The inability of the hydroxylated metabolites to enter the brain is most likely due to the high percentage of HHMC and HMMC conjugates in plasma, which are too polar to penetrate into the brain. Elmore et al. (Elmore *et al.*, 2017) showed that methylone, MDC, and HHMC were substrate-type releasers at monoamine transporters *in vitro*, but only methylone and MDC produced significant elevations in brain extracellular dopamine and 5-HT when administered *in vivo*. Thus, HHMC, in its unconjugated form, is able to serve as a monoamine transporter substrate, but this metabolite does not normally reach the brain after systemic methylone administration.

A secondary aim of the present study was to relate pharmacodynamic effects of methylone to brain concentrations of the drug and its metabolites, especially MDC, since this is the main metabolite reaching the brain. The behavioral scoring method that was used to assess

JPET Fast Forward. Published on March 30, 2021 as DOI: 10.1124/jpet.121.000531
This article has not been copyedited and formatted. The final version may differ from this version.

locomotor activation is sensitive to dose-dependent changes in behavior induced by stimulant drugs in rats (Elmore *et al.*, 2017). Methylone produced dose-dependent increases in forward locomotion, rearing, and patterned sniffing, consistent with previous reports of its stimulant effects in rats (López-Arnau *et al.*, 2013; Elmore *et al.*, 2017; Štefková *et al.*, 2017; Javadi-Paydar *et al.*, 2018). We found that behavioral scores were positively correlated with brain methylone and MDC concentrations at both time points examined, suggesting these analytes could contribute to motor stimulation. Effects of methylone on core temperature were more complex, characterized by acute hypothermia followed by a delayed, albeit modest, hyperthermia. The effects of methylone administration on body temperature were positively correlated with brain methylone and MDC at 40 min, but less so at 120 min. In a previous study, Elmore et al. (Elmore *et al.*, 2017) failed to find any correlation between core temperature and methylone or metabolite concentrations in plasma after 3, 6, or 12 mg/kg s.c. injections. Stefkova et al. (Štefková *et al.*, 2017) observed that methylone significantly increases colonic temperature in individually-housed and group-housed rats after s.c. doses of 10 and 20 mg/kg, and the effects are maintained for more than an hour. Javadi-Paydar et al. (Javadi-Paydar *et al.*, 2018) observed a modest but sustained hyperthermia (0.4-0.8ºC) for 4 hours after 10 mg/kg methylone in male rats. Overall, methylone appears to induce modest and sustained hyperthermia in rats, but this effect is influenced by dose and specific experimental conditions.

Perhaps the most important finding in the present report is the acute depletion of brain 5-HT produced by methylone administration. The effects of methylone on tissue 5-HT were dose- and time-dependent, such that the drug produced a delayed decrease in post-mortem tissue 5-HT in the frontal cortex but not striatum. The acute effects of methylone on tissue 5-HT reported here are similar to the effects reported for MDMA (Baumann *et al.*, 2007). Previous research has

JPET Fast Forward. Published on March 30, 2021 as DOI: 10.1124/jpet.121.000531
This article has not been copyedited and formatted. The final version may differ from this version.

demonstrated that methylone is a non-selective substrate-type releaser at the transporters for dopamine, norepinephrine, and 5-HT (Baumann *et al.*, 2013; Eshleman *et al.*, 2013; Simmler *et al.*, 2013)**.** Like other synthetic cathinones, methylone releases monoamine transmitters from intracellular stores via reversal of normal transporter flux (i.e., reverse transport). The results provided here show that the releasing actions of methylone may lead to acute depletion of intracellular stores of transmitter, but this effect is selective for 5-HT since post-mortem dopamine concentrations are actually increased and not depleted. The 5-HT depleting action of methylone seems to be exacerbated as time passes, since the most robust effects are observed after 2 hours. We have no explanation for why methylone produces selective decreases in cortical 5-HT, but such reductions could have functional consequences. In animal models, low cerebrospinal fluid concentrations of the 5-HT metabolite, 5-HIAA, and reduced 5-HT levels or turnover in the brain are associated with increased aggressive behavior (Nelson and Chiavegatto, 2001). In human case studies, methylone overdose is sometimes associated with aggressive and psychotic behaviors, and our preclinical findings suggest that decreased cortical 5-HT might contribute to such adverse effects (Diestelmann *et al.*, 2018).

In summary, we report the pharmacokinetics of methylone and its three major metabolites in brain and plasma of male rats. Methylone and MDC freely penetrate the blood-brain barrier, whereas HHMC and HMMC do not. Thus, hydroxylated metabolites of methylone do not contribute to centrally mediated pharmacodynamic effects. Methylone and MDC exhibit non-linear kinetics in the brain when assessed 120 min after methylone administration, suggesting delayed accumulation into neurons. Locomotor activity score is positively correlated with brain concentrations of methylone and MDC, while post-mortem levels of 5-HT in the frontal cortex are negatively correlated with these analytes. Taken together, our findings indicate

JPET Fast Forward. Published on March 30, 2021 as DOI: 10.1124/jpet.121.000531
This article has not been copyedited and formatted. The final version may differ from this version.

that non-linear accumulation of methylone and MDC in the brain could cause untoward effects on 5-HT neurons in vulnerable brain regions, including the frontal cortex.

JPET Fast Forward. Published on March 30, 2021 as DOI: 10.1124/jpet.121.000531
This article has not been copyedited and formatted. The final version may differ from this version.

Conflict of Interest

No author has an actual or perceived conflict of interest with the contents of this article.

Authorship Contributions

Participated in research design: Baumann, Concheiro

Conducted experiments: Centazzo, Chojnacki, Baumann, Elmore, Rodriguez, Acosta

Contributed new reagents or analytical tools: Suzuki, Rice, Concheiro

Performed data analysis: Centazzo, Baumann, Concheiro

Wrote or contributed to the writing of the manuscript: Centazzo, Baumann, Concheiro

References

Baumann M, Raley T, Partilla J, and Rothman R (1993) Biosynthesis of dopamine and serotonin in the rat brain after repeated cocaine injections: a microdissection mapping study. *Synapse* **14**:40–50.

Baumann MH, Ayestas MA, Partilla JS, Sink JR, Shulgin AT, Daley PF, Brandt SD, Rothman RB, Ruoho AE, and Cozzi N V. (2012) The designer methcathinone analogs, mephedrone and methylone, are substrates for monoamine transporters in brain tissue. *Neuropsychopharmacology* **37**:1192–1203, Nature Publishing Group.

Baumann MH, Partilla JS, and Lehner KR (2013) Psychoactive "bath salts": Not so soothing. *Eur J Pharmacol* **698**:1–5.

Baumann MH, Walters HM, Niello M, and Sitte HH (2018) Neuropharmacology of Synthetic Cathinones. *Handb Exp Pharmacol* **252**:113–142.

Baumann MH, Wang X, and Rothman RB (2007) 3,4-Methylenedioxymethamphetamine (MDMA) neurotoxicity in rats: A reappraisal of past and present findings. *Psychopharmacology (Berl)* **189**:407–424.

Cawrse BM, Levine B, Jufer RA, Fowler DR, Vorce SP, Dickson AJ, and Holler JM (2012) Distribution of methylone in four postmortem cases. *J Anal Toxicol* **36**:434–439.

De Felice LJ, Glennon RA, and Negus SS (2014) Synthetic Cathinones: Chemical Phylogeny, Physiology, and Neuropharmacology. *Life Sci* **97**:20–26.

Diestelmann M, Zangl A, Herrle I, Koch E, and Graw M (2018) MDPV in forensic routine cases: Psychotic and aggressive behavior in relation to plasma concentrations. *Forensic Sci Int* **283**:72-84.

de la Torre R, Farré M, Roset P, Pizarro N, Abanades S, Segura M, Segura J, and Camí J (2004) Human pharmacology of MDMA: pharmacokinetics, metabolism, and disposition. *Ther Drug Monit* **26**:137–44.

Drug Enforcement Administration (DEA) (2019) 3,4-Methylenedioxymethcathinone (Methylone).

Drug Enforcement Administration (DEA) (2013) Schedules of controlled substances: Placement of methylone into schedule I. *Fed Regist* **78**:21818–21825.

Ellefsen KN, Concheiro M, Suzuki M, Rice KC, Elmore JS, Baumann MH, and Huestis MA (2015) Quantification of methylone and metabolites in rat and human plasma by liquid chromatography-tandem mass spectrometry. *Forensic Toxicol* **33**:202–212.

Elmore JS, Dillon-Carter O, Partilla JS, Ellefsen KN, Concheiro M, Suzuki M, Rice KC, Huestis MA, and Baumann MH (2017) Pharmacokinetic Profiles and Pharmacodynamic Effects for Methylone and Its Metabolites in Rats. *Neuropsychopharmacology* **42**:649–660.

Eshleman AJ, Wolfrum KM, Hatfield MG, Johnson RA, Murphy K V., and Janowsky A (2013) Substituted methcathinones differ in transporter and receptor interactions. *Biochem Pharmacol* **85**:1803–1815.

Gannon BM, Galindo KI, Mesmin MP, Rice KC, and Collins GT (2018) Reinforcing Effects of Binary Mixtures of Common Bath Salt Constituents: Studies with 3,4-Methylenedioxypyrovalerone (MDPV), 3,4-Methylenedioxymethcathinone (methylone), and Caffeine in Rats. *Neuropsychopharmacology* **43**:761-769.

Gannon BM, Mesmin MP, Sulima A, Rice KC and Collins GT (2019) Behavioral economic analysis of the reinforcing effects of "bath salts" mixtures: studies with MDPV, methylone, and caffeine in male Sprague-Dawley rats (2019) Psychopharmacology **236**:1031-1041.

Grecco GG, Kisor DF, Magura JS, and Sprague JE (2017) Impact of common clandestine structural modifications on synthetic cathinone "bath salt" pharmacokinetics. *Toxicol Appl Pharmacol* **328**:18–24.

Javadi-Paydar M, Nguyen JD, Vandewater SA, Dickerson TJ, and Taffe MA (2018) Locomotor and Reinforcing Effects of Pentedrone, Pentylone and Methylone in Rats. *Neuropharmacology* **134**:57–64.

Kamata HT, Shima N, Zaitsu K, Kamata T, Miki A, Nishikawa M, Katagi M, and Tsuchihashi H (2006) Metabolism of the recently encountered designer drug, methylone, in humans and rats. *Xenobiotica* **36**:709–723.

López-Arnau R, Martínez-Clemente J, Carbó M, Pubill D, Escubedo E, and Camarasa J (2013) An integrated pharmacokinetic and pharmacodynamic study of a new drug of abuse, methylone, a synthetic cathinone sold as "bath salts." *Prog Neuro-Psychopharmacology Biol Psychiatry* **45**:64–72, Elsevier Inc.

Luethi D, Kolaczynska KE, Walter M, Suzuki M, Rice KC, Blough BE, Hoener MC, Baumann MH, and Liechti ME (2019) Metabolites of the ring-substituted stimulants MDMA, methylone and MDPV differentially affect human monoaminergic systems. *J Psychopharmacol* **33**:831–841.

Malpass A, White JM, Irvine RJ, Somogyi AA, and Bochner F (1999) Acute toxicity of 3,4-methylenedioxymethamphetamine (MDMA) in Sprague-Dawley and Dark Agouti rats. *Pharmacol Biochem Behav* **64**:29-34.

Madras BK (2016) The Growing Problem of New Psychoactive Substances (NPS), in *Neuropharmacology of New Psychoactive Substances (NPS). Current Topics in Behavioral Neurosciences.* (Baumann MH, Glennon R, and Wiley J eds) pp 1–18, Springer.

Meyer MR, Wilhelm J, Peters FT, and Maurer HH (2010) Beta-keto amphetamines: Studies on the metabolism of the designer drug mephedrone and toxicological detection of mephedrone, butylone, and methylone in urine using gas chromatography - Mass spectrometry. *Anal Bioanal Chem* **397**:1225–1233.

Nelson RJ and Chiavegatto S (2001) Molecular basis of aggresion. *Trends Neurosci* **24(12)**:713-719.

Oliver CF, Palamar JJ, Salomone A, Simmons SJ, Philogene-Khalid HL, Stokes-McCloskey N, and Rawls SM (2019) Synthetic cathinone adulteration of illegal drugs. *Psychopharmacology (Berl)* **236**:869–879, Psychopharmacology.

Pedersen AJ, Petersen TH, and Linnet K (2013) In vitro metabolism and pharmacokinetic studies on methylone. *Drug Metab Dispos* **41**:1247–1255.

Schindler CW, Thorndike EB, Goldberg SR, Lehner KR, Cozzi N V., Brandt SD, and Baumann MH (2016) Reinforcing and neurochemical effects of the "bath salts" constituents 3,4-methylenedioxypyrovalerone (MDPV) and 3,4- methylenedioxy-N-methylcathinone (methylone) in male rats. *Psychopharmacology (Berl)* **233**:1981–1990.

Simmler LD, Buser TA, Donzelli M, Schramm Y, Dieu LH, Huwyler J, Chaboz S, Hoener MC, and Liechti ME (2013) Pharmacological characterization of designer cathinones in vitro. *Br J Pharmacol* **168**:458–470.

Štefková K, Židková M, Horsley RR, Pinterová N, Šíchová K, Uttl L, Balíková M, Danda H, Kuchar M, and Páleníček T (2017) Pharmacokinetic, ambulatory, and hyperthermic effects of 3,4-methylenedioxy-n-methylcathinone (Methylone) in rats. *Front Psychiatry* **8**:1–11.

Vanderwater SA, Creehan KM, and Taffe MA (2015) Intravenous self-administration of entactogen-class stimulants in male rats. *Neuropharmacology* **99**:538–545.

Watterson LR, Hood L, Sewalia K, Tomek SE, Yahn S, Johnson CT, Wegner S, Blough BE, Marusich JA, and Olive MF (2012) The Reinforcing and Rewarding Effects of Methylone, a Synthetic Cathinone Commonly Found in "Bath Salts." *J Addict Res Ther* **Supple 9**:002.

Footnotes

The research program of Dr. Baumann is generously supported by the Intramural Research Program (IRP) of the National Institute on Drug Abuse (NIDA, National Institutes of Health (NIH), grant# DA000523-13.

JPET Fast Forward. Published on March 30, 2021 as DOI: 10.1124/jpet.121.000531
This article has not been copyedited and formatted. The final version may differ from this version.

Figure legends

Fig. 1. Metabolism of methylone, showing chemical structures of methylone and its main metabolites 3,4-dihydroxy-*N*-methylcathinone (HHMC), 4-hydroxy-3-methoxy-*N*-methylcathinone (HMMC), and 3,4-methylenedioxycathinone (MDC).

Fig. 2. Plasma and brain concentrations of methylone and 3,4-methylenedioxycathinone (MDC) at early and late time points (40 min and 120 min) after s.c. methylone injections (6, 12, and 24 mg/kg). Data are mean ± SEM for n=8 rats/group.

Fig. 3. Plasma and brain concentrations of 3,4-dihydroxy-*N*-methylcathinone (HHMC) and 4-hydroxy-3-methoxy-*N*-methylcathinone (HMMC) at early and late time points (40 min and 120 min) after s.c. methylone injections (6, 12, and 24 mg/kg). Data are mean ± SEM for n=8 rats/group.

Fig. 4. Predicted versus observed brain concentrations of methylone and 3,4-methylenedioxycathinone (MDC) at early and late time points (40 min and 120 min). Predicted concentrations at the 12 and 24 mg/kg doses were calculated by multiplying the observed values at 6 mg/kg by a factor of 2 and 4, respectively. Data are mean ± SEM for n=8 rats/group. Asterisks represent significant difference compared to predicted group.

Fig. 5. Effects of s.c. methylone administration (6, 12, and 24 mg/kg dose) on body temperature and behavioral score at 40 min and 120 min post-injection. Data are mean ± SEM for n=8 rats/group. Asterisks represent significant differences compared to saline-treated control group.

Fig. 6. Effect of s.c. methylone administration (6, 12, and 24 mg/kg) on post-mortem levels of dopamine (DA) and serotonin (5-HT) from frontal cortex at 40 min and 120 min post-injection. Data are mean ± SEM for n=8 rats/group. Asterisks represent significant differences compared to saline-treated control group.

Fig. 7. Effect of s.c. methylone administration (6, 12, and 24 mg/kg) on post-mortem levels of dopamine (DA) and serotonin (5-HT) from dorsal striatum at 40 min and 120 min post-injection. Data are mean ± SEM for n=8 rats/group. Asterisks represent significant differences compared to saline-treated control group.

Fig. 8. Correlations between brain methylone concentrations and body temperature or behavioral score at 40 min and 120 min post-injection.

Fig. 9. Correlations between brain 3,4-methylenedioxycathinone (MDC) concentrations and body temperature or behavioral score at 40 min and 120 min post-injection.

Fig. 10. Correlations between brain methylone concentrations and frontal cortical 5-HT and dopamine (DA) at 40 min and 120 min post-injection.

JPET Fast Forward. Published on March 30, 2021 as DOI: 10.1124/jpet.121.000531
This article has not been copyedited and formatted. The final version may differ from this version.

Fig. 11. Correlations between brain MDC concentrations and frontal cortical 5-HT and dopamine (DA) at 40 min and 120 min post-injection.

JPET Fast Forward. Published on March 30, 2021 as DOI: 10.1124/jpet.121.000531
This article has not been copyedited and formatted. The final version may differ from this version.

Tables

Table 1. Plasma concentrations (ng/mL) of methylone, 3,4-methylenedioxycathinone (MDC), 3,4-dihydroxy-*N*-methylcathinone (HHMC) and 4-hydroxy-3-methoxy-*N*-methylcathinone (HMMC) from rats receiving s.c. methylone at 6, 12, and 24 mg/kg. Samples were collected at 40 or 120 min post-injection. Data are mean ± SEM for N=8 rats/group.

Dose (mg/kg)	Collection time (min)	Methylone (ng/mL)	MDC (ng/mL)	HHMC (ng/mL)	HMMC (ng/mL)
6	40	687.4±37	234.6±10.8	290±22.6	201.6±12.5
	120	133.4±9.4	164±10.7	157.9±12.8	248.5±41.8
12	40	1,037.3±27.6	491.7±17.5	432.8±55	244.5±17
	120	506.5±40.2	384.5±12.6	260±36.7	334.8±30.4
24	40	3,749.9±132.2	1,007.6±34.5	809.8±71.2	402.9±16.8
	120	1,230.8±196.5	875.3±31.1	686.7±45.6	537.8±38.8

JPET Fast Forward. Published on March 30, 2021 as DOI: 10.1124/jpet.121.000531
This article has not been copyedited and formatted. The final version may differ from this version.

Table 2. Brain concentrations (ng/g) of methylone, 3,4-methylenedioxycathinone (MDC), 3,4-dihydroxy-*N*-methcathinone (HHMC) and 4-hydroxy-3-methoxy-*N*-methcathinone (HMMC) from rats receiving s.c. methylone at 6, 12, and 24 mg/kg collected at 40 or 120 min post-injection. Data are mean ± SEM for N=8 rats/group.

Dose (mg/kg)	Collection time (min)	Methylone (ng/g)	MDC (ng/g)	HHMC (ng/g)	HMMC (ng/g)
6	40	5404.6±779	857±122.7	3.9±1	16.8±1.7
	120	403.7±62.3	545.4±80.9	1.1±0.8	13.9±1.8
12	40	14,357.3±1324.4	2,832.5±437.7	12±1.9	25.7±4
	120	2,796.8±704.5	2,441±303.4	9.4±1.8	34.5±4.1
24	40	36,222.9±5617.2	4,886.5±770.3	30.3±3.5	54.1±6.6
	120	13,671.8±1339.3	4,750.2±406.3	23.8±3.5	59.7±7.6

JPET Fast Forward. Published on March 30, 2021 as DOI: 10.1124/jpet.121.000531
This article has not been copyedited and formatted. The final version may differ from this version.

Table 3. Brain-to-plasma concentration ratios for methylone, 3,4-methylenedioxycathinone (MDC), 3,4-dihydroxy-*N*-methylcathinone (HHMC) and 4-hydroxy-3-methoxy-*N*-methylcathinone (HMMC) from rats receiving s.c. methylone at 6, 12, and 24 mg/kg. Data are mean ± SEM for N=8 rats/group.

Dose (mg/kg)	Collection time (min)	Methylone	MDC	HHMC	HMMC
6	40	7.66±0.76	3.76±0.64	0.01±0	0.08±0.01
	120	3±0.4	3.34±0.46	0.01±0	0.06±0.01
12	40	14±1.44	5.77±0.86	0.03±0.01	0.11±0.02
	120	5.4±1.08	6.35±0.76	0.04±0.01	0.1±0.01
24	40	9.64±1.37	4.88±0.80	0.07±0.03	0.20±0.09
	120	12.39±1.72	5.48±0.52	0.04±0.01	0.12±0.02

JPET Fast Forward. Published on March 30, 2021 as DOI: 10.1124/jpet.121.000531
This article has not been copyedited and formatted. The final version may differ from this version.

Centazzo et al., Figure 1

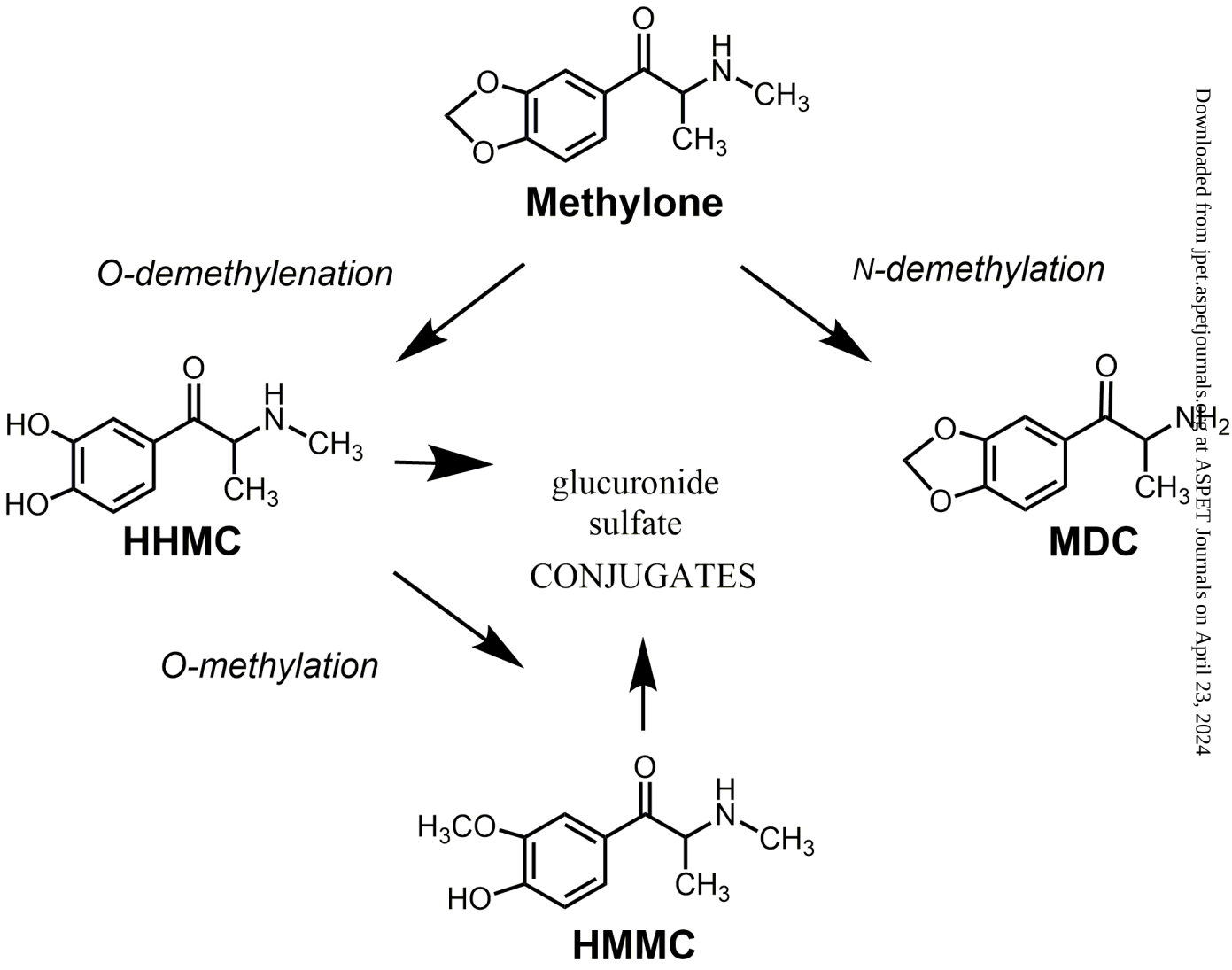

JPET Fast Forward. Published on March 30, 2021 as DOI: 10.1124/jpet.121.000531
This article has not been copyedited and formatted. The final version may differ from this version.

Centazzo et al., Figure 2

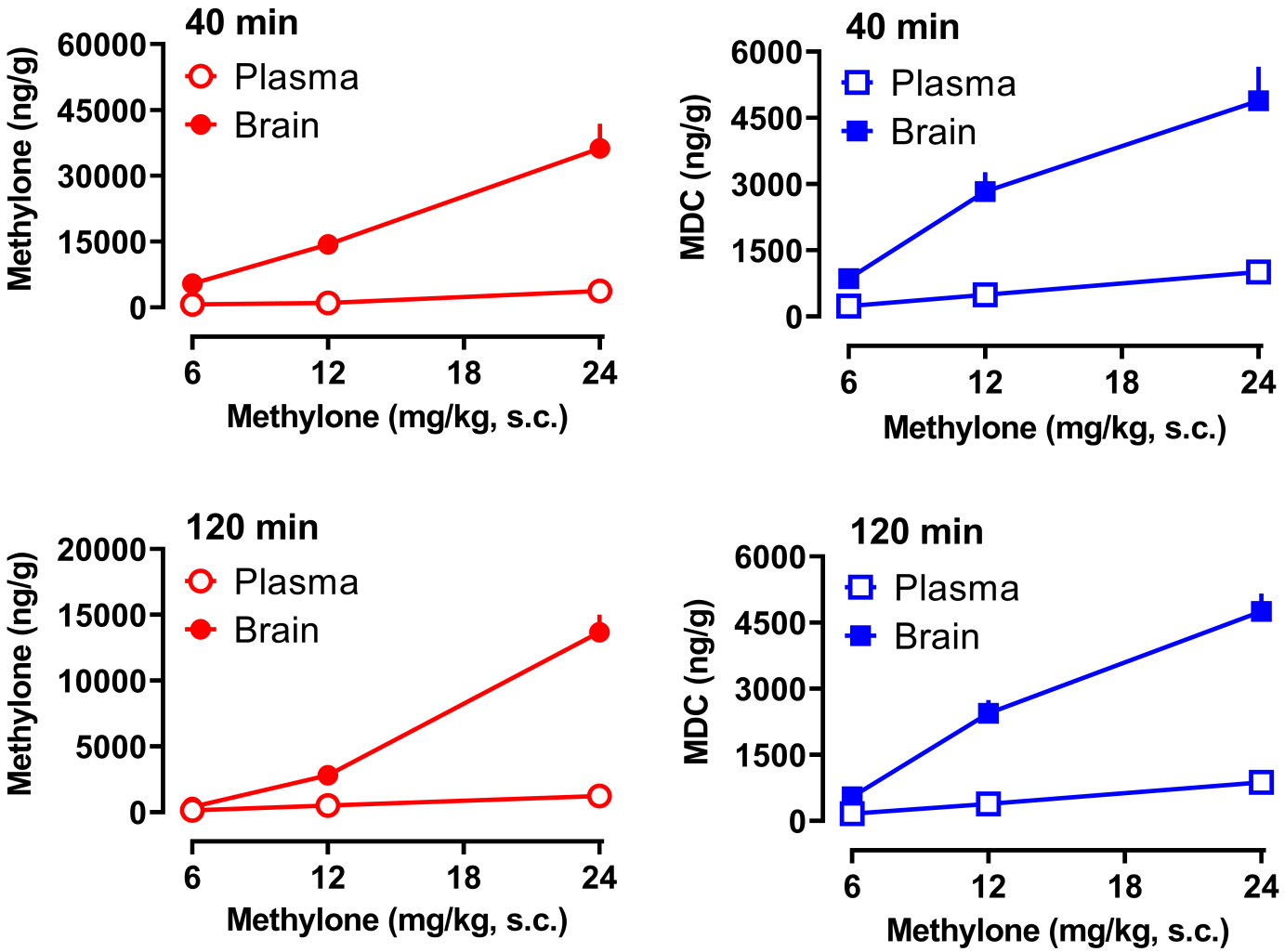

JPET Fast Forward. Published on March 30, 2021 as DOI: 10.1124/jpet.121.000531
This article has not been copyedited and formatted. The final version may differ from this version.

Centazzo et al., Figure 3

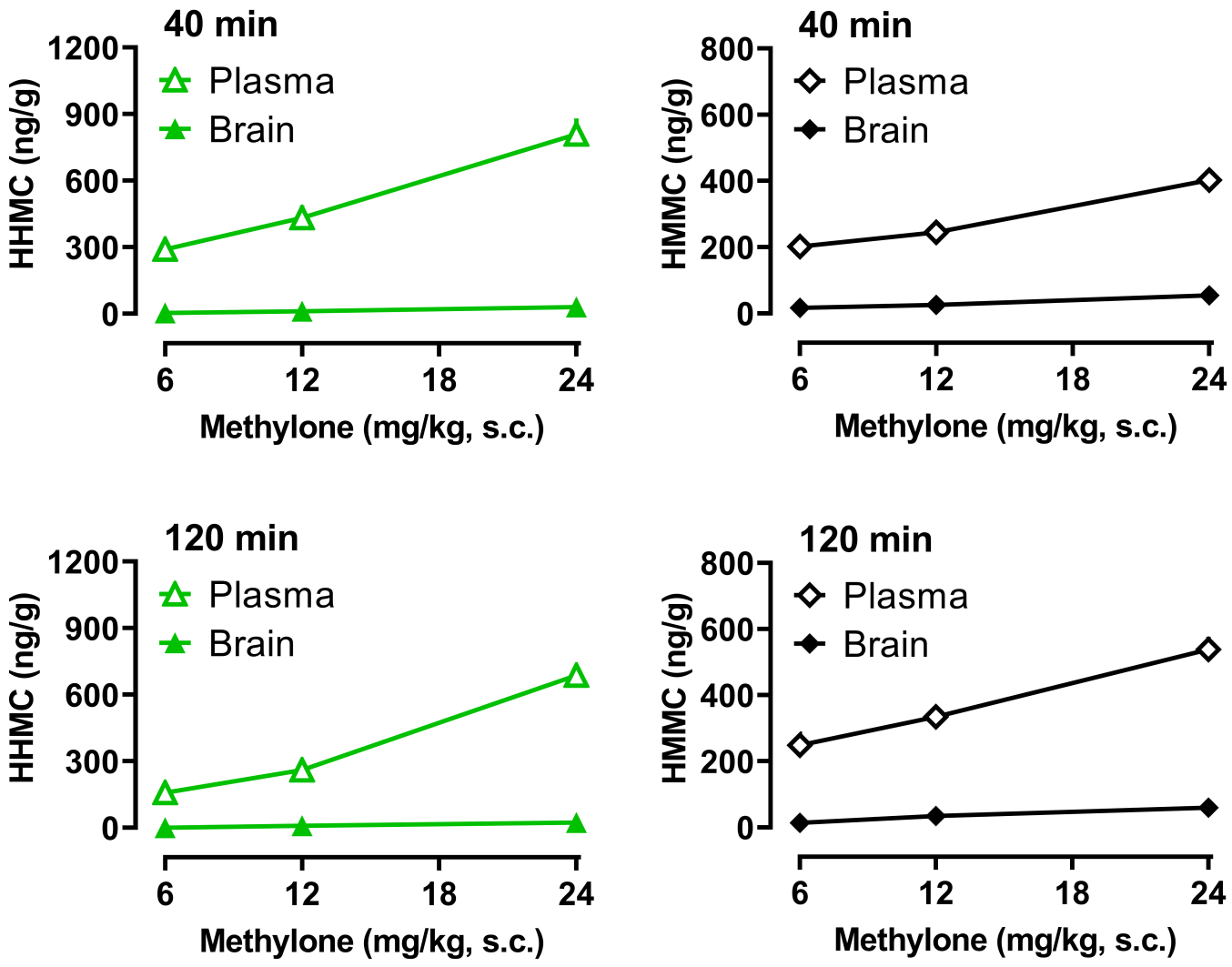

JPET Fast Forward. Published on March 30, 2021 as DOI: 10.1124/jpet.121.000531
This article has not been copyedited and formatted. The final version may differ from this version.

Centazzo et al., Figure 4

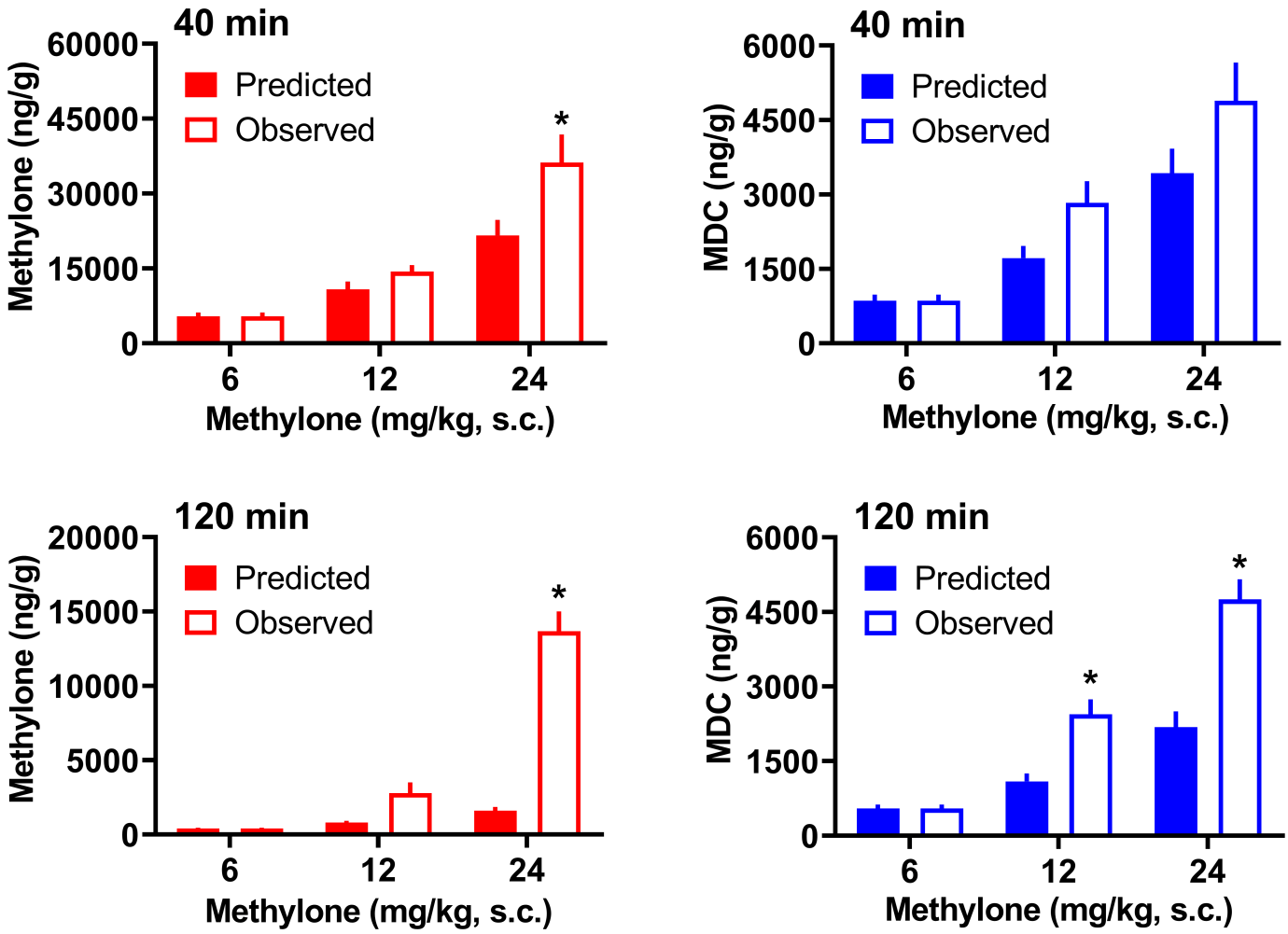

JPET Fast Forward. Published on March 30, 2021 as DOI: 10.1124/jpet.121.000531
This article has not been copyedited and formatted. The final version may differ from this version.

Centazzo et al., Figure 5

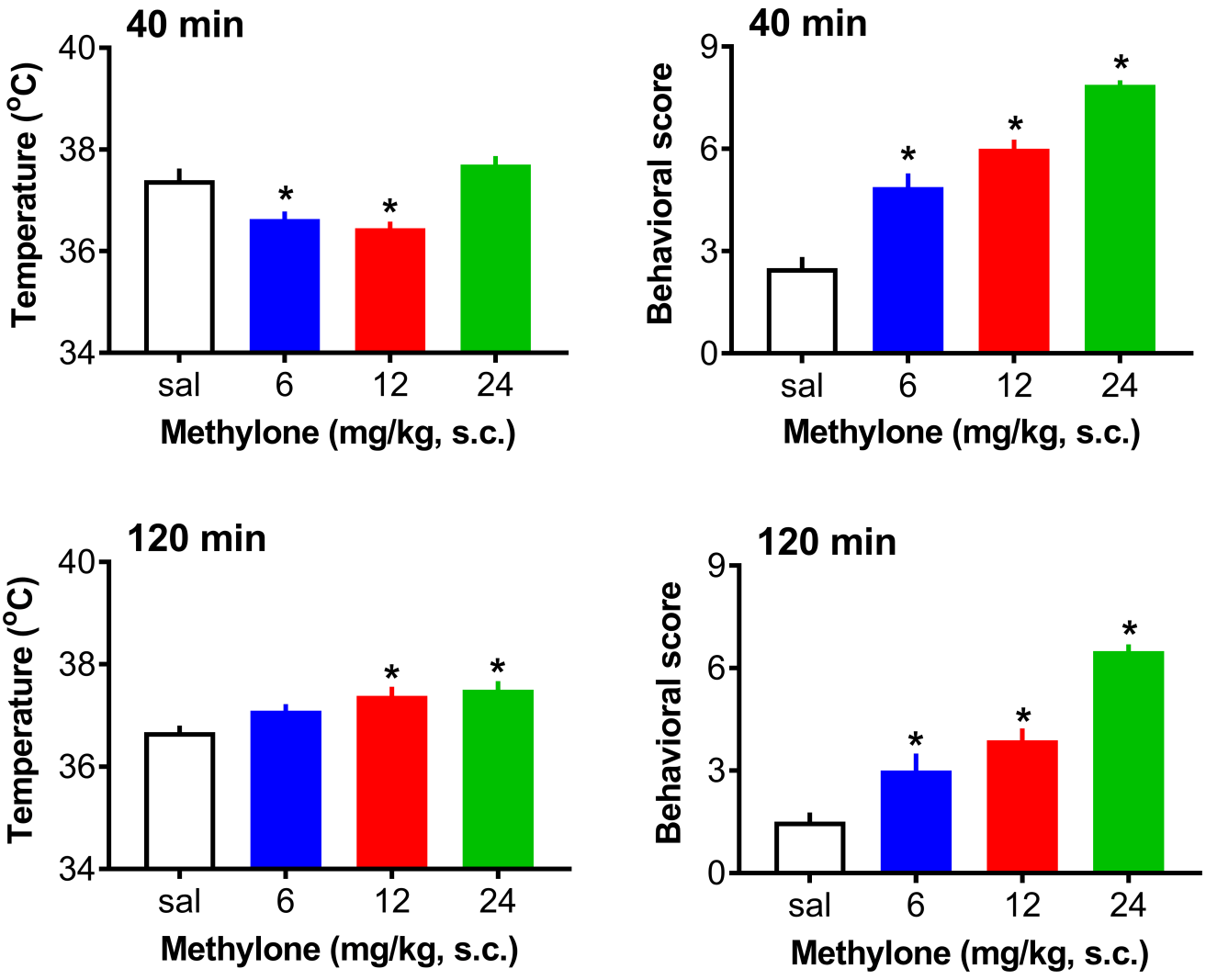

JPET Fast Forward. Published on March 30, 2021 as DOI: 10.1124/jpet.121.000531
This article has not been copyedited and formatted. The final version may differ from this version.

Centazzo et al., Figure 6

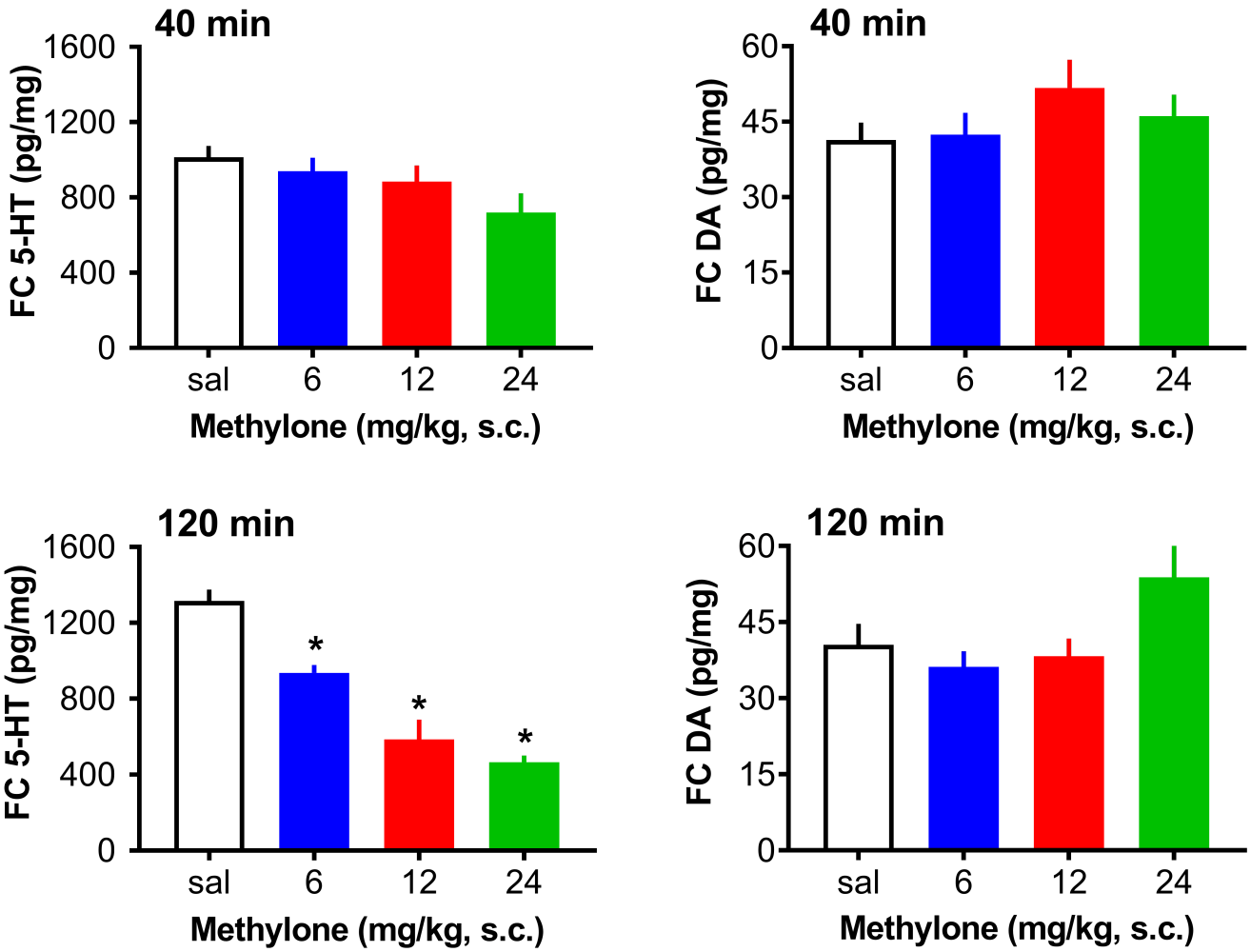

JPET Fast Forward. Published on March 30, 2021 as DOI: 10.1124/jpet.121.000531
This article has not been copyedited and formatted. The final version may differ from this version.

Centazzo et al., Figure 7

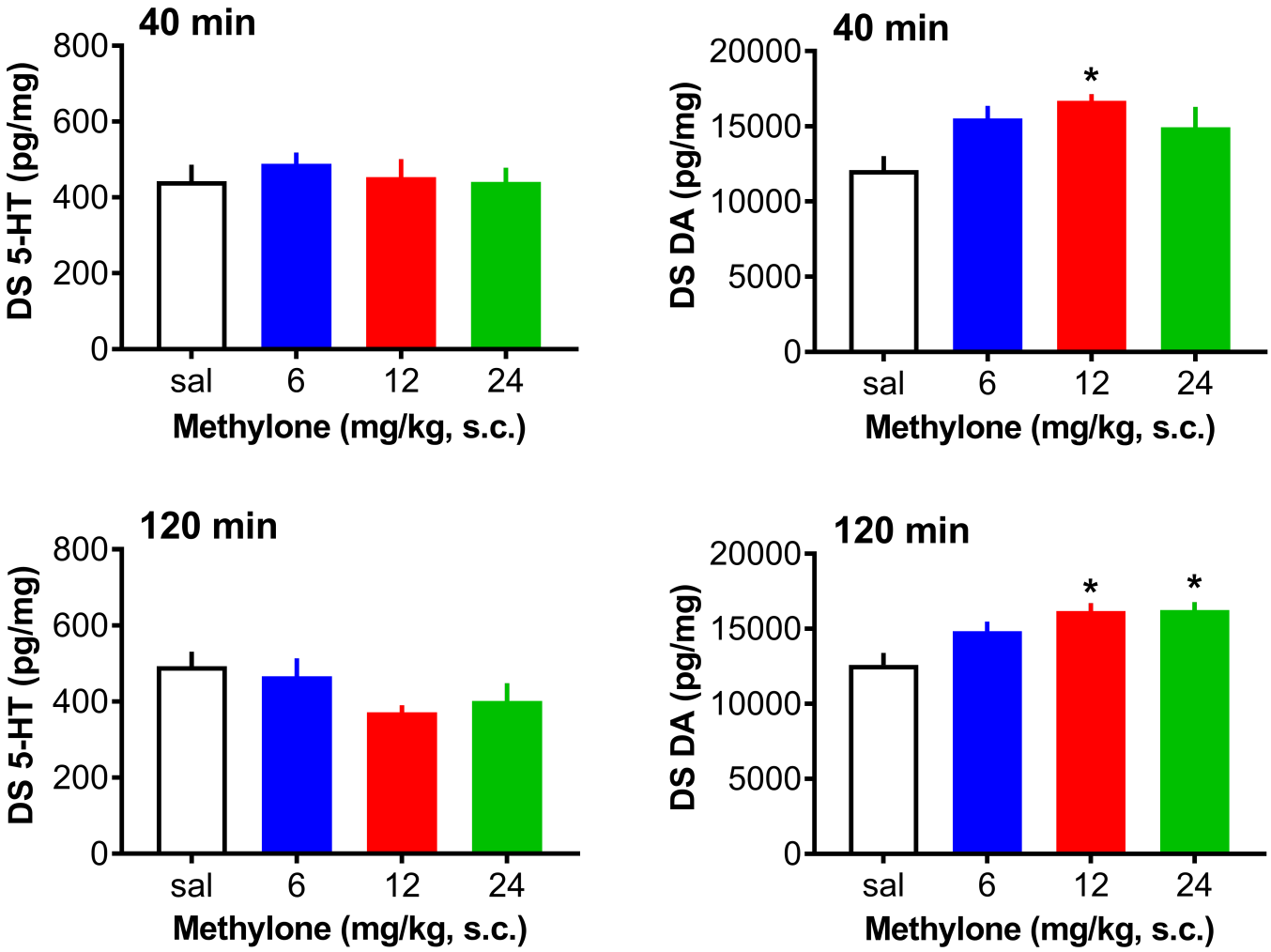

JPET Fast Forward. Published on March 30, 2021 as DOI: 10.1124/jpet.121.000531
This article has not been copyedited and formatted. The final version may differ from this version.

Centazzo et al., Figure 8

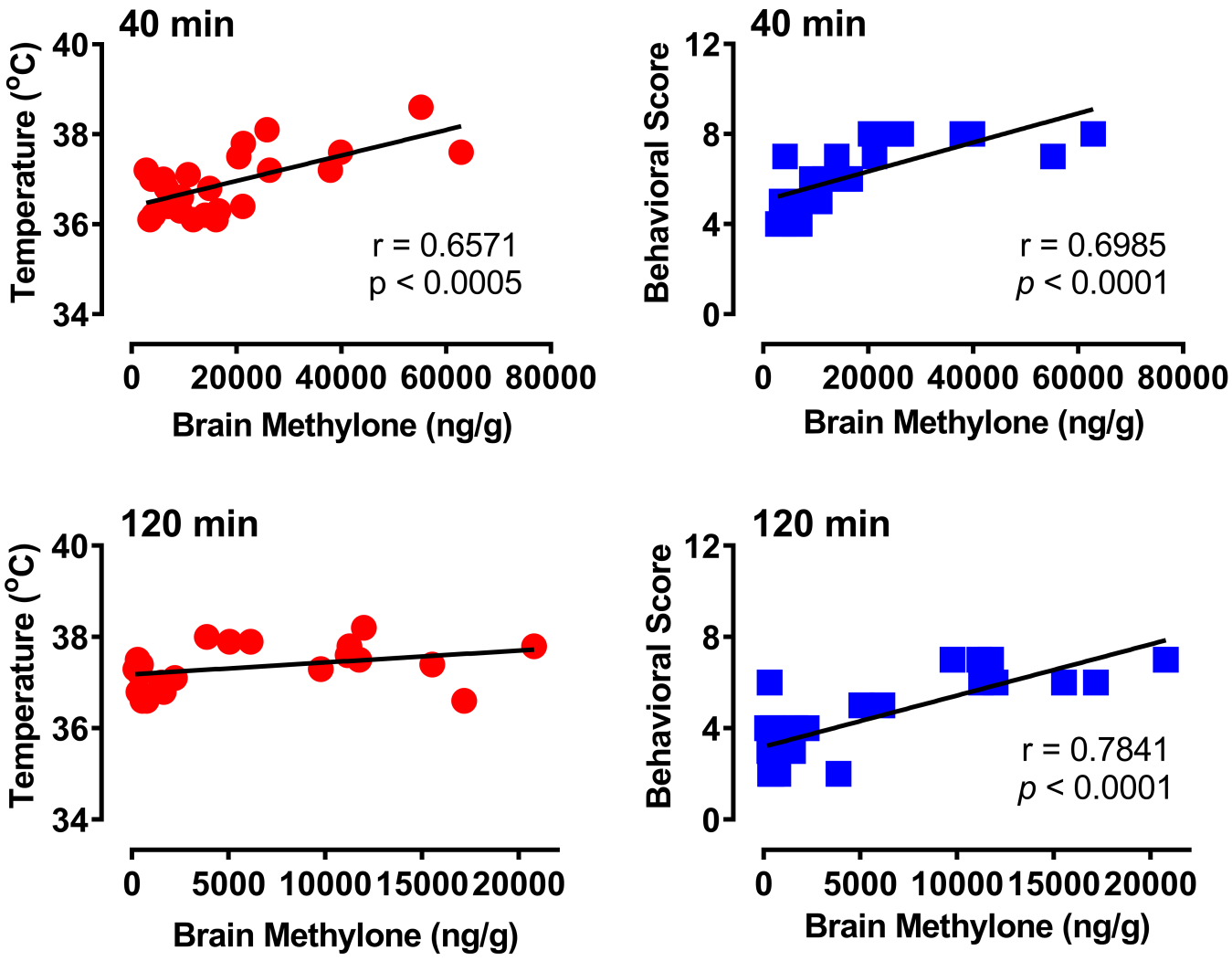

JPET Fast Forward. Published on March 30, 2021 as DOI: 10.1124/jpet.121.000531
This article has not been copyedited and formatted. The final version may differ from this version.

Centazzo et al., Figure 9

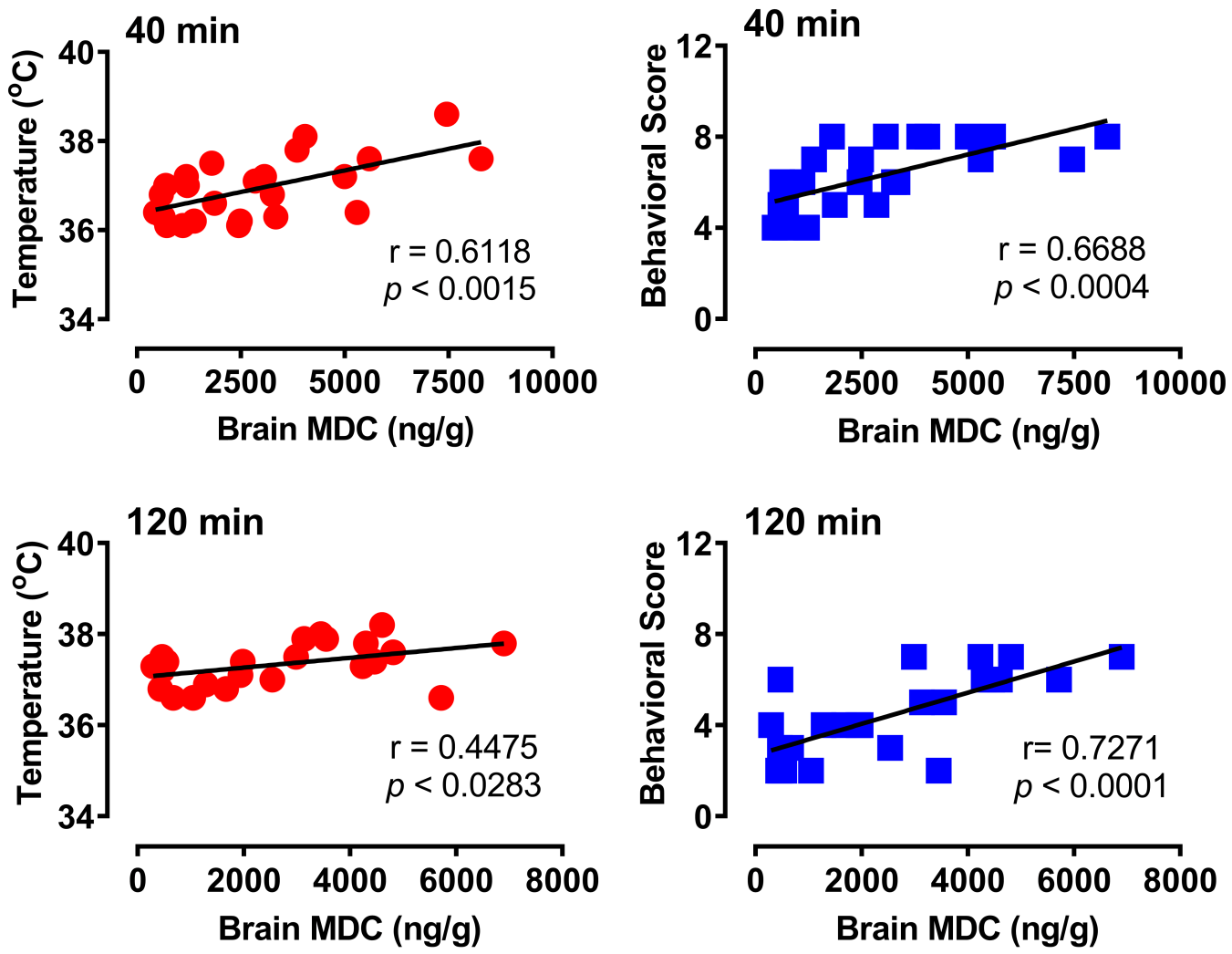

JPET Fast Forward. Published on March 30, 2021 as DOI: 10.1124/jpet.121.000531
This article has not been copyedited and formatted. The final version may differ from this version.

Centazzo et al., Figure 10